HHS Public Access

Author manuscript

Biochim Biophys Acta. Author manuscript; available in PMC 2019 March 01.

Published in final edited form as:

Biochim Biophys Acta. 2018 March ; 1860(3): 645–653. doi:10.1016/j.bbamem.2017.11.016.

Human Bile Acid Transporter ASBT (*SLC10A2*) Forms Functional Non-Covalent Homodimers and Higher Order Oligomers

Paresh P. Chothe, **Lindsay C Czuba**, **Robyn H. Moore**, and **Peter W. Swaan***

Department of Pharmaceutical Sciences, School of Pharmacy, University of Maryland, 20 Penn Street, Baltimore, MD 21201, USA

Abstract

The human apical sodium-dependent bile acid transporter, hASBT/*SLC10A2*, plays a central role in cholesterol homeostasis via the efficient reabsorption of bile acids from the distal ileum. hASBT has been shown to self-associate in higher order complexes, but while the functional role of endogenous cysteines has been reported, their implication in the oligomerization of hASBT remains unresolved. Here, we determined the self-association architecture of hASBT by site-directed mutagenesis combined with biochemical, immunological and functional approaches. We generated a cysteine-less form of hASBT by creating point mutations at all 13 endogenous cysteines in a stepwise manner. Although Cysless hASBT had significantly reduced function correlated with lowered surface expression, it featured an extra glycosylation site that facilitated its differentiation from wt-hASBT on immunoblots. Decreased protein expression was associated with instability and subsequent proteasome-dependent degradation of Cysless hASBT protein. Chemical cross-linking of wild-type and Cysless species revealed that hASBT exists as an active dimer and/or higher order oligomer with apparently no requirement for endogenous cysteine residues. This was further corroborated by co-immunoprecipitation of differentially tagged (HA-, Flag-) wild-type and Cysless hASBT. Finally, Cysless hASBT exhibited a dominant-negative effect when co-expressed with wild-type hASBT which validated heterodimerization/oligomerization at the functional level. Combined, our data conclusively demonstrate the functional existence of hASBT dimers and higher order oligomers irrespective of cysteine-mediated covalent bonds, thereby providing greater understanding of its topological assembly at the membrane surface.

Graphical Abstract

*Corresponding Author: Peter W. Swaan, Ph.D., Department of Pharmaceutical Sciences, University of Maryland, 20 Penn Street, HSF2-543, Baltimore, MD 21201 USA, Tel: (410) 706-0103, Fax: (410) 706-5017, pswaan@rx.umaryland.edu.

5.1. Conflict of Interest

The authors declare no conflict of interest

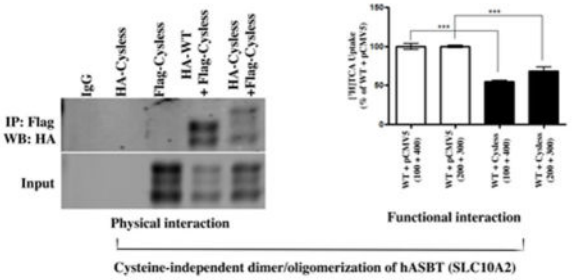

Keywords

Bile acid; transporter; epitope tag; intestinal absorption

1.1 Introduction

Bile acids (BAs) are secreted, after a meal, from the gall bladder into the small intestine to aid in the absorption of lipids and fat-soluble nutrients [1, 2]. Whereas most BAs are reabsorbed as mixed micelles with dietary lipids, the human apical sodium-dependent bile acid transporter (hASBT, *SLC10A2*), predominantly expressed in the distal ileum, facilitates the reabsorption of up to 95% of the remaining BAs, thereby efficiently preventing their excretion in the feces. BAs are then returned to the liver via the portal circulation mediated by the basolateral bile acid exporter OSTα-OSTβ [1, 3]. Subsequently, the paralogous bile acid transporter NTCP (*SLC10A1*) enables bile acid reentry into the liver. Both ASBT and NTCP have been extensively studied in regards to their relevance to bile acid handling [1, 4], cholesterol homeostasis[5, 6], and drug delivery applications [7, 8]. The recent appreciation that BAs can function as complex signaling molecules that modulate glucose, lipid and energy metabolism [9, 10] further necessitates a deeper understanding of BA homeostasis and the physiological role that transporters play in this process.

Our previous work sought to delineate the membrane topology and understand the molecular transport mechanism of hASBT-mediated transport [11–14]. hASBT contains 348 amino acids including 13 cysteines, 12 of which are conserved across mammalian species (Fig. 1). The structural and functional contributions of cysteines in membrane proteins, including transporters, have been well described: they play a role in conformational stability [15, 16] through intramolecular disulfide bonds as well as in protein oligomerization [17–19] via intermolecular disulfide linkage. Moreover, cysteine residues engaged in disulfide linkages have shown to be critical for intracellular protein trafficking, stability and –ultimately– for protein function [20, 21]. Our previous work suggested that Cys51, Cys105 and Cys255 are critical for hASBT function, while Cys74 may be implicated in protein trafficking [22]. However, the overall contribution of endogenous cysteines in the oligomeric assembly of functional hASBT is unclear. Previous work had suggested that hASBT presumably functions as a monomer, but that it may also exist in dimeric and higher order oligomeric forms [23, 24]. In fact, early studies by Kramer and co-workers [24] using photoaffinity labelling in rabbit intestine correlated a 93 kDa integral membrane protein with sodium-dependent bile acid uptake and this size is in line with a rabbit ASBT dimer. Other *SLC10A*

family members, i.e. *SLC10A1*, *SLC10A5* and *SLC10A7*, are known to form dimers as well [25–27]. In fact, it has been suggested that membrane transporters with fewer than 12 transmembrane domains may require oligomerization to be functional [28]. However, there is no direct evidence for hASBT to date to support this notion and the present study sought to close this gap in our understanding of its structure and function.

Given the important role of cysteine residues in maintaining protein structural integrity required for proper assembly and function, we aimed to investigate the relevance of native cysteines to the oligomerization of hASBT. In this report, we used mutational analysis combined with biochemical, immunological and functional approaches to examine the role of endogenous cysteines in the dimer and higher order oligomer formation of hASBT.

2.1. MATERIALS AND METHODS

2.2. Materials

^{3}H]-Taurocholic acid (TCA) was procured from Radiolabeled Chemicals, Inc, (St. Louis, MO). Taurocholic acid, tunicamycin, cyclosporin A (CsA) and dithiothreitol (DTT) were from Sigma (St. Louis, MO). MG132 was from Cayman Chemical (Ann Arbor, MI). EZ Link Sulfo-NHS-SS-biotin, maleimide-PEG$_{11}$-biotin, dithiobis[succinimidylpropionate] (DSP) and 3,3′-dithiobis[succinimidylpropionate] (DTSSP) were purchased from Pierce Biotechnology (Rockford, IL). Cell culture media and supplies were from Invitrogen (Rockville, MD). All other chemicals were of the highest purity available commercially. Goat polyclonal anti-hASBT antibody and Protein G PLUS-Agarose were from Santa Cruz Biotechnology Inc. (Santa Cruz CA). Mouse anti-Flag antibody was from LifeTein LLC (South Plainfield, NJ), mouse anti-HA and mouse anti-calnexin antibodies were from Sigma (St. Louis, MO).

2.3. Cell Culture and Transfection

COS-1 cells were cultured in Dulbecco's modification of Eagle's medium (DMEM) with 10% FBS, penicillin (100 IU/ml) and streptomycin (100 μg/ml) (Life Technologies, Inc., Rockville, MD). Transient DNA transfection in COS-1 cells was carried out using Turbofect (Thermo Scientific) transfection reagent according to manufacturer's directions. Briefly, COS-1 cells were seeded in 24-well plate at an initial density of 0.065×10^{6} cells per well. After 24 h, cells were transfected with WT or Cysless hASBT with Turbofect transfection reagent (1:4). 48 h post-transfection, cells were used for either uptake measurements or surface biotinylation and Western blot analysis.

2.4. Site-directed Mutagenesis

hASBT cDNA in pCMV5 vector was used as a template. Site-specific mutations at 13 cysteines to either alanine or threonine were introduced using a site-directed mutagenesis kit from Stratagene (La Jolla, CA). All mutant hASBT were confirmed by sequencing. Primers used for creating these mutations were obtained from our previous studies [22].

2.5. Uptake Assay and Transport Kinetic Measurements

COS-1 cells transiently transfected with WT and Cysless ASBT (48 h post-transfection) were used for uptake studies. Uptake was carried out as described previously [29]. Briefly, cells were washed twice with Dulbecco's Phosphate-Buffered Saline (containing calcium and magnesium) and then incubated at 37 °C for 12 min (TCA uptake is linear up to 15 min) [30] in Modified Hanks' balanced salt solution (MHBSS), pH 7.4, containing 5 μM cold TCA spiked with 1 μCi/ml [^{3}H]-TCA. Uptake was stopped by washing cells with ice-cold DPBS containing 0.2% BSA and 0.5 mM TCA. Cells were lysed in 350 μl of 1N NaOH, and radioactivity associated with cells was measured by liquid scintillation counting, using a LS6500 liquid scintillation counter (Beckmann Coulter, Inc., Fullerton, CA). Uptake rates were determined as nmoles per mg protein per 12 min. Protein was quantified using the Bradford assay.

To examine the effect of DTT on hASBT, COS-1 cells, transiently expressing hASBT, were pre-incubated with DTT (10 mM) for 20 min. Cells were then washed with uptake buffer twice followed by TCA uptake in the absence and presence of DTT.

Substrate kinetics for hASBT was analyzed by measuring the uptake with increasing concentrations of TCA (2.5 – 200 μM). The Michaelis-Menten-like constant (K_t) and maximal velocity (V_{max}) were determined, using GraphPad 5.0 (San Diego, CA), by fitting the Michaelis-Menten equation describing a single saturable transport system to the data: $v = V_{max} \cdot S/(K_t + S)$ where v is the uptake rate, S is the substrate concentration, K_t is the Michaelis-Menten-like constant, and V_{max} is the maximal transport velocity.

2.6. Western Blot and Surface Biotinylation

Cells were washed twice with ice-cold PBS and then solubilized in NP-40 lysis buffer (50mM Tris-HCI pH 8.0, 150mM NaCl and 1% NP-40) containing 1× complete protease inhibitor mixture (Roche applied Science). Protein concentrations were measured with the Bradford method. 35 μg of protein lysate was loaded and resolved with 10% SDS-PAGE. Proteins were transferred to PVDF membrane at 100v for 1h. Membranes were blocked in 2% non-fat dry milk in TBS followed by incubation with respective antibodies: goat anti-hASBT, mouse anti-HA, anti-Flag (1:1000), rabbit anti-cadherin and mouse anti-calnexin (1:3000). An Odyssey imaging system (Licor, NE) was used for visualizing protein bands.

For surface biotinylation, COS-1 cells transiently transfected with WT and Cysless hASBT were labeled with EZ Link NHS-SS-biotin reagent. The procedure was followed as described previously [29]. Briefly, cells were washed with ice cold DPBS twice and then incubated with EZ Link NHS-SS-biotin (1 mg/ml) for 30 min at 4 °C. The reaction was quenched with 1M Tris pH 7.4. Cells were disrupted in NP-40 lysis buffer followed by overnight incubation with streptavidin agarose beads at 4 °C. Beads were washed with TBS twice and then with NP-40 lysis buffer twice. Beads were incubated with Laemmli buffer for 40 min and then boiled for 10 min to release proteins from the beads. Finally, proteins were used for immunoblotting for the analysis of hASBT protein expression using goat anti-hASBT (1:1000). Labeling specificity to the cell membrane proteins was confirmed by the

absence of ER protein calnexin (90 kDa) and presence of a cell surface marker pan cadherin (120 kDa).

2.7. Protein Stability of Cysless hASBT

To determine whether protein folding or stability played a role in the expression of Cysless hASBT, transiently transfected COS-1 cells were incubated with the proteasome inhibitor MG132 (10μM, 6h) and the chemical chaperone CsA (25μM, 18h). At the end of the treatment, cells were washed twice with ice-cold PBS and used for surface biotinylation and Western blot analysis.

2.8. Chemical cross-linking

The method for chemical cross-linking was adopted from a previous report [31]. Briefly, COS-1 cells were transiently transfected with hASBT. 48 h post-transfection, cells were washed with PBS twice and incubated with DSP (0.5 mM) and DTSSP (2.5 mM) for 30 min at room temperature. The cross-linking reaction was terminated by adding 1M Tris pH 7.4 to a final concentration of 20 mM for 15 min. Cells were then washed with PBS twice and disrupted with NP-40 lysis buffer. Cell lysates were used for Western blot analysis using goat anti-ASBT antibody (1:1000).

2.9. Construction of HA-hASBT, Flag-hASBT, HA-Cysless hASBT and Flag-Cysless hASBT

HA (YPYDVPDYA) and Flag (DYKDDDDK) epitopes were inserted between N318 and K319 residues near the C-terminal of WT and cysless hASBT as described previously [22] by inverted PCR mutagenesis. Briefly, WT and Cysless hASBT in a pCMV5 vector were used as a template for mutagenesis reactions. All oligonucleotides were 5′-phosporylated. Primers for WT hASBT with HA and Flag insertions were: forward, 5′-GTGCCTGATTACGCCAAGGCAGAAATT CCAG-3′, reverse, 5′-GTCGTAAGGGTAGTTTTTTCCATGACA TTTC-3′ and forward, 5′-GATGACGACAAGAAGGCAGAAATTCCAG-3′, reverse, 5′-GTCCTTGTAGTCGTTTTTTCCATGACATTTC-3′, respectively. Forward primers for Cysless ASBT were identical to those above while reverse primers with HA and Flag insertion were: 5′-GTCGTAAGGGTAGTTTTTTCCATGAGCTTTC-3′ and 5′-GTCCTTGTAGTCGTTTTTTCCATGAGCTTTC-3′, respectively. The primers were designed so that half of the epitope sequence was incorporated into the 5′-end of each, the up- and downstream, primer. The PCR product was purified using a Qiagen kit (Chatsworth, CA) and resuspended in Tris-HCl (pH 8.5). The PCR product was then ligated using T4 DNA ligase (NEB, Beverly, MA) for 2 h at room temperature followed by heat inactivation at 65 °C for 10 min. The resulting product was digested with Dpn1 for 4 h to remove unreacted template DNA. XL 1 blue supercompetent cells were transformed with Dpn1 treated PCR product, plated on Luria-Bertani (LB) with ampicillin plates followed by incubation overnight at 37 °C. Plasmid minipreps were performed on selected colonies which were grown in LB broth. HA and Flag insertion was confirmed by DNA sequencing.

2.10. Immunoprecipitation

COS-1 cells were transiently transfected with differentially tagged WT and Cysless-hASBT as follows: HA-WT, Flag-WT, HA-WT + Flag-WT, HA-cysless, Flag-Cysless, HA-WT + Flag-Cysless, and HA-Cysless + Flag-Cysless. 48 h post-transfection cells were washed twice with ice-cold PBS and solubilized in NP-40 lysis buffer. 500 μg Cell extracts were precleaned with Protein G PLUS-Agarose for 1 hour at 4 °C. Supernatants were separated and incubated with 1 μg of either mouse anti-HA or anti-Flag antibody for 4 h at 4 °C followed by incubation with Protein G PLUS-Agarose at 4 °C overnight. IPs were washed with NP-40 lysis buffer four times and used for immunoblotting with either mouse anti-Flag or anti-HA antibody. Membrane was stripped with Gn-HCl stripping buffer (6M guanidine, 20mM Tris-HCl pH 7.5, 0.2% NP-40 and 0.1M β-mercaptoethanol) as previously described [32] and then probed with either mouse anti-Flag or anti-HA antibody for input analysis.

2.11. Data analysis

Statistical analysis was carried out using one-way analysis of variance (ANOVA) with Dunnett's post-hoc test. $P < 0.05$ was taken as statistically significant. Experiments were performed at least three times, and measurements were made in triplicate for each experimental condition. Data are presented as means ± SE.

3.1. RESULTS

3.2. Generating a Cysless hASBT Mutant by Site-directed Mutagenesis

hASBT contains 13 endogenous cysteines. Cys51, Cys105, Cys132 and Cys270 are fully conserved in hASBT and its liver paralog hNTCP (Figure 1). 12 out of the 13 residues are conserved among ASBTs across other species (Fig. 1). Only Cys105 and Cys106 were found conserved in the bacterial putative homologues of Asbt from *Neisseria meningitidis* (nmAsbt), while only Cys255 was found to be conserved in the putative Asbt homologue from *Yersinia frederiksenii* (yfAsbt). Each cysteine in hASBT was consecutively mutated to either alanine or threonine by site-directed mutagenesis as described under 'Materials and Methods'. The order of mutation and the choice of amino acid for replacement were based on our previous study [22]. The cysteines with lower impact on hASBT function were mutated first followed by residues previously shown to affect protein function or membrane expression.

3.3. Cysless hASBT Retains Membrane Expression, Loses Function, and Gains an *N*-Glycosylation Site

WT and Cysless hASBT were transiently transfected in COS-1 cells and then evaluated for their transport function and surface expression by determining [^{3}H]-TCA uptake and cell surface biotinylation, respectively. In parallel experiments, the protein levels of both ASBT species in whole (total) cell lysate was analyzed in order to determine the effect of cysteine mutations on stability, putative degradation and membrane insertion of the protein. Uptake rates of both WT and Cysless hASBT were normalized to their respective cell surface expression. Cysless hASBT completely lost function compared to WT (Fig. 2A). Since hASBT protein features one glycosylation site (Asn^{10}) it is typically visualized as its core

glycosylated (~41 kDa) and non-glycosylated (~ 37 kDa) forms. Surprisingly, Cysless hASBT revealed an extra band (~45 kDa) just above the core glycosylated form (Figure 2B). The additional 3kDa molecular weight increase suggested that Cysless hASBT is glycosylated at more than one site. To test the hypothesis that the C7T mutation might have introduced an additional *N*-glycosylation epitope at Asn^5 (based on the consensus sequence N-X-S/T), we treated COS-1 cells, expressing Cysless hASBT, with the *N*-linked glycosylation inhibitor tunicamycin (10μg/ml for 24 h) and analyzed the glycosylation status of WT and Cysless hASBT by Western blot. For WT hASBT, the core glycosylated band disappeared as expected, yielding only non-glycosylated hASBT protein (Figure 2C). Similarly, the putative extra-glycosylated and core glycosylated bands disappeared upon tunicamycin treatment of Cysless hASBT (Figure 2C), suggesting that this mutant is glycosylated at more than one asparagine site, likely Asn^5 in addition to Asn^{10}. Importantly, this mutant provided us with a valuable tool in our subsequent studies: visualization of the extra-glycosylated band can be used to differentiate Cysless hASBT when co-expressed with WT ASBT (Figs. 5 & 6).

3.4. Cysless hASBT is Properly Folded but Quickly Degraded by the Proteasome

Cysteines play a crucial role in proper folding, trafficking, membrane insertion and stability of a protein. Since mutation of all 13 endogenous cysteines caused a significant reduction in total as well as cell surface hASBT protein expression (Figure 2B), we investigated the effect of chemical chaperone cyclosporin A (assists in protein folding) [33, 34] and the proteasome inhibitor MG132 on total cellular and membrane surface protein expression of Cysless hASBT. CsA was unable to rescue Cysless hASBT expression, indicating that its decreased expression was likely not due to protein misfolding; however, MG132 significantly increased surface and total expression of Cysless hASBT (Fig. 3), suggesting that proteosomal degradation plays a role in hASBT protein expression and stability.

3.5. Chemical Cross-linking Shows hASBT Dimeric and Higher Order Oligomeric Architecture

In order to assess whether hASBT can adopt an oligomeric structure we used a well-established chemical cross-linking protocol using two thiol-cleavable, lipophilic and bifunctional cross-linkers: cell permeable DSP and cell impermeable DTSSP, both containing a cleavable disulfide bond in their 8 carbon (12Å) spacer arm. First, we determined the oligomerization status of hASBT under non-reducing (control) and reducing conditions with DTT, a compound known to cleave both intra- and inter-molecular disulfide bonds involved in sulfhydryl cross-linking. Under control conditions (no cross-linker present), hASBT was found predominantly in monomeric and dimeric forms with an apparent molecular weight of ~37 kDa and ~74 kDa respectively. Surprisingly, the dimer was intact even in the presence of DTT (Fig. 4A, lane 3), suggesting strong protein-protein interactions that could not be attributed to disulfide linkages. This is further corroborated by the observation that DTT treatment had a minimal, yet statistically significant inhibitory (~24%) effect on hASBT-mediated TCA uptake (Fig. 4B), suggesting that disulfide-linked residues do not play a role in hASBT transport function.

After treatment with DSP, hASBT was detected in aggregated form at >250 kDa (Fig. 4A, lane 4); contrarily, upon DTSSP exposure hASBT was present in either dimeric or higher order oligomeric forms (Fig. 4A, lane 6). The total absence (lane 4) and minimally detectable level (lane 6) of hASBT monomer upon treatment with DSP and DTSSP, respectively, and the abundant presence of higher molecular weight species (lanes 5 and 7) under reducing conditions suggested successful cross-linking.

To establish the functional status of hASBT dimers/oligomers as a consequence of chemical cross-linking, substrate uptake was determined in the absence and presence of DSP and DTSSP. As shown in Fig. 4C, DSP but not DTSSP, significantly decreased (~75%) [^{3}H]-TCA uptake by hASBT. This suggests that the dimer and higher order oligomers resulting from DTSSP treatment are fully functional; in contrast, DSP treatment causes hASBT to form high molecular weight oligomers and aggregates while simultaneously significantly reducing hASBT transport function.

3.6. hASBT Forms Homodimers

To further delineate hASBT dimerization/oligomerization and the potential role (or lack thereof) of endogenous cysteines, we performed co-immunoprecipitation using differentially HA- and FLAG-tagged WT and Cysless hASBT (i.e. HA-WT, Flag-WT, HA-Cysless and Flag-Cysless hASBT). Although both HA and Flag-tagged proteins were functionally active, insertion of the Flag epitope had a more adverse effect on hASBT function compared to the HA epitope (Fig. 5A). This could be attributed to the highly charged nature of the FLAG epitope in contrast to the more neutral HA tag given that both were inserted at the C-terminus which plays a role in membrane targeting and insertion of hASBT protein [25]. Next, the physical interaction between HA- and Flag-tagged WT-hASBT was assessed by transfecting COS-1 cells with either HA-WT and Flag-WT alone, or together. Upon immunoprecipitation with anti-Flag antibody followed by immunoblotting with anti-HA antibody we found that both HA- and Flag-hASBT interacted with each other (Fig. 5B, top panel). The blot was stripped and re-probed with anti-Flag antibody for input analysis (Fig. 5B, bottom panel), showing antibody specificity (Full blots are shown in supplemental data S1). The presence of hASBT dimers and higher order oligomers was also observed in these blots (supplemental data). After demonstrating homodimerization of hASBT using differentially tagged forms of WT protein (Fig. 5B), we subsequently assessed the requirement of native cysteines in this process by determining the physical interaction between WT and Cysless hASBT and, between two Cysless hASBT species. Our data show that Flag-Cysless hASBT interacted with HA-WT hASBT (Figure 5C, lane 4) as well as HA-Cysless hASBT (Figure 5C, lane 5). The blot was stripped and then re-probed with anti-Flag antibody for input analysis (Figure 5C, bottom panel). In parallel experiments, the same cell lysates used for Figs 5B and 5C were subjected to reverse immunoprecipitation using anti-HA antibody followed by Western blot analysis with anti-Flag antibody (Figure 5D, top panel), and for analyzing the combinations of HA-WT and Flag-Cysless as well as HA-Cysless and Flag-Cysless (Figure 5E, top panel). For input and specificity analysis, blots were stripped and re-probed with anti-HA antibody (Figure 5D and E, bottom panel). Combined, these data convincingly demonstrate cysteine-independent homodimerization of hASBT.

3.7. Functional Evidence for hASBT Dimer/Oligomerization upon Co-expression with its Cysless Mutant

To determine hASBT dimer/oligomerization at the functional level, we co-expressed HA-WT along with Cysless hASBT in COS-1 cells anticipating that nonfunctional Cysless hASBT would have a dominant negative effect on functional HA-WT. We used HA-tagged WT hASBT to effectively differentiate it from Cysless hASBT when both forms are expressed and detected at the plasma membrane. Due to its lower surface expression, Cysless hASBT was transfected at relatively higher DNA amounts than HA-WT hASBT (ratio HA-WT:Cysless hASBT 2:3 and 1:4); however, total DNA content was kept constant during transfection. First, we determined the effect of co-expression of pCMV5 (vector control) and Cysless hASBT on the transport activity of HA-WT hASBT, showing a dose-dependent reduction in [^{3}H]-TCA uptake in the presence of Cysless hASBT but not pCMV5 control (Fig. 6A). Simultaneously, we determined that membrane expression of HA-WT hASBT protein was not affected when co-expressed with Cysless hASBT (Fig. 6B). Interestingly, membrane expression of HA-WT hASBT was much lower when co-transfected with Cysless hASBT at the 1:4 ratio (Fig. 6B, lane 3) in comparison to the 2:3 ratio (lane 4), which can likely be attributed to the relatively lower DNA amounts of HA-WT hASBT (100 ng) in combination with a dominant-negative effect of Cysless hASBT on HA-WT expression upon heteromerization.

To further confirm the functional heteromerization between WT and Cysless hASBT, COS-1 cells expressing HA-WT hASBT and co-transfected with either pCMV5 vector or Cysless hASBT at a ratio of 2:3 HA-WT:Cysless/pCMV5 were used to assess TCA substrate kinetics (Fig. 6C). This ratio was selected since surface expression of HA-WT remains intact at detectable level in the presence of Cysless hABST (Figure 6B). The K_t values for HA-WT hASBT in the presence of pCMV5 and Cysless hASBT were 22.85 ± 1.47 μM and 25.01 ± 5.52 μM respectively while V_{max} values were 7.38 ± 0.14 and 3.94 ± 0.17 nmol/mg protein/12 min respectively. The presence of Cysless hASBT severely affected the maximum velocity of HA-WT hASBT by 46% with apparently no effect on affinity (Figure 6C). These observations are consistent with the co-transfection of a non-functional and functional form of hASBT as this theoretically would affect its V_{max} due to a decline in the number of functional transporter molecules available at the cell surface but not its K_t, which would vary only if conformational changes in the binding/transport domains of WT-hASBT occurred upon heteromerization with Cysless hASBT. These data not only highlight functional dimer/oligomerization of HA-WT with Cysless hASBT but also that individual subunits of hASBT dimers are functional. Further, these results validate our previous observation that hASBT exists as an active dimer and/or oligomer that does not require endogenous cysteines [35].

4.1. DISCUSSION

There is increasing evidence that major facilitator superfamily proteins can self-assemble within the plasma membrane as functional homodimers or higher order oligomeric structures [36–40]. In the present study we explored the membrane assembly status of hASBT and demonstrated that this protein exists as a functional homodimer and higher order oligomer independent of endogenous cysteines (Figs. 4–6). The role of endogenous cysteines in the

oligomerization process was investigated by stepwise construction of a hASBT variant that had all 13 endogenous cysteine residues (Fig. 1) mutated to either alanine or threonine. The resulting Cysless protein was thoroughly evaluated with respect to its transport function, membrane expression, folding and stability (Figs. 2, 3). As expected from our previous work emphasizing the critical importance of several cysteine residues for hASBT function [22], Cysless hASBT completely lost function along with impaired membrane surface expression. To further assess the mechanism behind this severely lowered hASBT surface expression we found that the chemical chaperone cyclosporin A, commonly used to aid proper protein folding of mutants [33, 34] could not salvage protein expression of Cysless hASBT, thus signifying the importance of endogenous cysteines to the overall stability of hASBT protein. However, the proteasome inhibitor MG132 effectively rescued membrane and total protein expression of Cysless hASBT, suggesting that Cysless protein is quickly destined for proteasomal degradation. This observation was not surprising as recent work by our laboratory and others [41, 42] established that hASBT protein under basal levels has a short half-life due to rapid degradation via the ubiquitin-proteasome pathway.

During the process of generating a Cysless hASBT protein, we found that introduction of a threonine mutation at Cys7 introduced an extra *N*-linked glycosylation site at Asn^5 (Fig. 2). The resulting extra-glycoslyated band for Cysless hASBT afforded us with the advantage of subsequently differentiating this species on Western blots from other engineered forms of the protein (e.g. WT or HA/Flag-tagged). Next, we used a multi-tiered approach to determine the oligomeric status of hASBT including crosslinking, co-immunoprecipitation and functional assays.

Chemical crosslinking with bifunctional crosslinking reagents has been used successfully to determine and characterize functional protein complexes of membrane transporters [25, 31]. We demonstrate that hASBT spontaneously adopts an active dimer and higher order oligomer structure (Fig. 4A) when incubated with the amine-reactive, homobifunctual crosslinker DSP and its water-soluble, membrane impermeable analog, DTSSP. The effect of the cell permeable cross-linker DSP on hASBT oligomerization appears to be non-specific as the protein is exclusively found in an aggregated form (molecular weight ≥250kDa) with significantly reduced function (Fig. 4C); the remaining activity is likely due to trace amounts present of either monomer, dimer or higher order oligomers (Fig. 4A, lane 4). In contrast, hASBT treated under the same conditions with the membrane impermeant cross-linker DTSSP retained activity (Figure 4C). To our surprise, hASBT appeared not only as a monomer but also as a dimer in control experiments (no cross-linkers) even under reducing conditions, suggesting that hASBT homodimerization (but not higher order oligomerization) may not require inter- and/or intra-molecular cross-linking. Analogously, we show that the reduction agent DTT had a minimal (yet, statistically significant) effect on hASBT function (Fig. 4B), which may explain the absence of inter- or intra-molecular disulfide linkage. Accordingly, we conclude that hASBT is likely functionally active as a monomer, dimer and/or higher order oligomers. These data further corroborate early *in vivo* studies by Kramer and colleagues [24] who detected a ~93kDa bile acid transporting protein (roughly comparable to an ASBT dimer) in rabbit intestine upon photoaffinity labeling with specific, photoreactive bile acid analogs. Analogously, Bijmans and co-workers [25] detected a band

at ~100kDa corresponding to NTCP dimer (ASBT's hepatic paralog) upon treatment of rat liver membranes with chemical cross-linkers.

Though cross-linkers have been used successfully in determining protein oligomerization, data interpretation can be complicated by their relative lack of specificity for the target protein (as we encountered during DSP treatment). Therefore, we set to further validate cross-linking results by immunoprecipitation and co-expression of WT and Cysless hASBT both individually tagged with either HA or Flag epitopes. Co-immunoprecipitation data strongly suggest a physical association between differentially tagged WT hASBT and Cysless hASBT molecules (Fig. 5), thereby further substantiating the dimeric architecture of hASBT observed during crosslinking (Fig. 4A). Formation of hASBT heterodimers and/or hetero-oligomers does not require native cysteines, which suggests that it may rely on hydrophobic interactions between different regions of hASBT protein, such as transmembrane helices. The GXXXG (X=any amino acid) and GXXXA motifs are commonly found in α-helices of transmembrane proteins and have important implications in the association of adjacent helices [43–45] as well as protein-protein interactions [46–48]. Indeed, we have previously identified the presence of multiple GXXXG motifs in hASBT [49], in particular the regions between Gly^{197} to Gly^{212} and Gly^{237} to Ala^{248} that are rich in small hydrophobic residues spaced at intervals corresponding to one α-helical rise (Fig. 1). We found that Cys mutation of Gly^{197} and Ile^{208} abrogated function, whereas Gly^{201} and Gly^{212} retained less than 10% activity upon cysteine mutation. Accordingly, we speculated that these residues play an important role in protein stability; however, combined with our present finding that Cys residues do not play a role in hASBT dimerization, future studies will explore the role of the GXXXG motif in promoting hASBT self-association.

Finally, we confirmed functional activity of dimerized/oligomerized WT and Cysless hASBT (Fig. 6) and observed that non-functional Cysless hASBT exhibited a dominant-negative effect on WT hASBT function. This effect was not due to compromised membrane expression but resulted from a specific physical interaction between the two protein species (Fig. 6A, B). This strategy has been used previously to understand the homodimerization of several transporter proteins [50]. Additionally, kinetic analysis unambiguously established the functional co-operation between WT and Cysless ASBT, since non-functional Cysless ASBT significantly reduced maximum transport velocity (V_{max}) without affecting transport affinity (K_t) of WT ASBT. Absent of intra-molecular association via S-S linkages (which would require endogenous cysteines) we conclude that hydrophobic interactions between different transmembrane helices or intra/extracellular domains might serve as a driving force for the observed heterodimerization/oligomerization of hASBT, similar to previously reported interactions with BCRP (*ABCG2*) [51], DAT (*SLC6A3*) [50] and MRP1 (*ABCC1*) [31, 52]. Based on crystal packing data, the structures of putative bacterial hASBT homologues nmAsbt and yfAsbt were not suggested to form a dimer or higher order oligomers [53, 54], but this might be attributed to their vast evolutionary distance from hASBT as demonstrated by Lionarons and colleagues [55]. Further studies will address the participation of individual transmembrane helices and/or other structural domains in the dimerization/oligomerization of hASBT protein.

In summary, the present study provides evidence for the homodimeric and/or homo-oligomeric architecture of hASBT based on a dominant negative Cysless hASBT construct, chemical crosslinking, and co-immunoprecipitation. We conclusively show that endogenous cysteines are not involved in this process, even though they are critical for the membrane expression, stability and function of hASBT. Our study provides new support for Bijsman's hypothesis that homodimerization could be a common phenomenon in the *SLC10A* protein family. Furthermore, we provide important new information on the functional mechanism and regulation of a key protein involved in cholesterol and energy metabolism.

Supplementary Material

Refer to Web version on PubMed Central for supplementary material.

Acknowledgments

6.1. Funding

The research was funded by the National Institutes of Health, Institute of Diabetes, Digestive Diseases & Kidney grant # DK56631 to PWS

We sincerely thank Dr. Sairam Mallajosyula for the critical discussions regarding hASBT topology and the dimer model.

Abbreviations

COS-1	monkey kidney fibroblast cell line
CsA	Cyclosporin A
Cysless	Cysteineless
DSP	dithiobis[succinimidylpropionate]
DTSSP	3,3′-dithiobis[succinimidylpropionate]
DTT	Dithiothreitol
hASBT	human apical sodium-dependent bile acid transporter
NTCP	Na^+taurocholate co-transporting polypeptide
OST	organic solute transporter
PAGE	polyacrylamide gel electrophoresis
TM	transmembrane

References

1. Dawson PA. Role of the intestinal bile acid transporters in bile acid and drug disposition. Handb Exp Pharmacol. :169–203.
2. Hofmann AF, Hagey LR. Bile Acids: Chemistry, Pathochemistry, Biology, Pathobiology, and Therapeutics. Cell Mol Life Sci. 2008; 65:2461–2483. [PubMed: 18488143]

3. Alrefai WA, Gill RK. Bile acid transporters: structure, function, regulation and pathophysiological implications. Pharm Res. 2007; 24:1803–1823. [PubMed: 17404808]
4. Shneider BL. Intestinal bile acid transport: biology, physiology, and pathophysiology. J Pediatr Gastroenterol Nutr. 2001; 32:407–417. [PubMed: 11396803]
5. West KL, McGrane M, Odom D, Keller B, Fernandez ML. SC-435, an ileal apical sodium-codependent bile acid transporter inhibitor alters mRNA levels and enzyme activities of selected genes involved in hepatic cholesterol and lipoprotein metabolism in guinea pigs. J Nutr Biochem. 2005; 16:722–728. [PubMed: 16169202]
6. West KL, Zern TL, Butteiger DN, Keller BT, Fernandez ML. SC-435, an ileal apical sodium co-dependent bile acid transporter (ASBT) inhibitor lowers plasma cholesterol and reduces atherosclerosis in guinea pigs. Atherosclerosis. 2003; 171:201–210. [PubMed: 14644388]
7. Balakrishnan A, Polli JE. Apical sodium dependent bile acid transporter (ASBT, SLC10A2): a potential prodrug target. Mol Pharm. 2006; 3:223–230. [PubMed: 16749855]
8. Zheng X, Polli JE. Synthesis and in vitro evaluation of potential sustained release prodrugs via targeting ASBT. Int J Pharm. 396:111–118.
9. Claro da Silva T, Polli JE, Swaan PW. The solute carrier family 10 (SLC10): beyond bile acid transport. Molecular aspects of medicine. 2013; 34:252–269. [PubMed: 23506869]
10. Watanabe M, Houten SM, Mataki C, Christoffolete MA, Kim BW, Sato H, Messaddeq N, Harney JW, Ezaki O, Kodama T, Schoonjans K, Bianco AC, Auwerx J. Bile acids induce energy expenditure by promoting intracellular thyroid hormone activation. Nature. 2006; 439:484–489. [PubMed: 16400329]
11. Zhang EY, Phelps MA, Banerjee A, Khantwal CM, Chang C, Helsper F, Swaan PW. Topology scanning and putative three-dimensional structure of the extracellular binding domains of the apical sodium-dependent bile acid transporter (SLC10A2). Biochemistry. 2004; 43:11380–11392. [PubMed: 15350125]
12. Hussainzada N, Banerjee A, Swaan PW. Transmembrane domain VII of the human apical sodium-dependent bile acid transporter ASBT (SLC10A2) lines the substrate translocation pathway. Mol Pharmacol. 2006; 70:1565–1574. [PubMed: 16899538]
13. Banerjee A, Swaan PW. Membrane topology of human ASBT (SLC10A2) determined by dual label epitope insertion scanning mutagenesis. New evidence for seven transmembrane domains. Biochemistry. 2006; 45:943–953. [PubMed: 16411770]
14. Hussainzada N, Khandewal A, Swaan PW. Conformational flexibility of helix VI is essential for substrate permeation of the human apical sodium-dependent bile acid transporter. Mol Pharmacol. 2008; 73:305–313. [PubMed: 17971420]
15. Mamathambika BS, Bardwell JC. Disulfide-linked protein folding pathways. Annu Rev Cell Dev Biol. 2008; 24:211–235. [PubMed: 18588487]
16. Trivedi MV, Laurence JS, Siahaan TJ. The role of thiols and disulfides on protein stability. Curr Protein Pept Sci. 2009; 10:614–625. [PubMed: 19538140]
17. Hebert DN, Carruthers A. Cholate-solubilized erythrocyte glucose transporters exist as a mixture of homodimers and homotetramers. Biochemistry. 1991; 30:4654–4658. [PubMed: 2029513]
18. Brast S, Grabner A, Sucic S, Sitte HH, Hermann E, Pavenstadt H, Schlatter E, Ciarimboli G. The cysteines of the extracellular loop are crucial for trafficking of human organic cation transporter 2 to the plasma membrane and are involved in oligomerization. FASEB J. 26:976–986.
19. Kage K, Fujita T, Sugimoto Y. Role of Cys-603 in dimer/oligomer formation of the breast cancer resistance protein BCRP/ABCG2. Cancer Sci. 2005; 96:866–872. [PubMed: 16367905]
20. Stitham J, Gleim SR, Douville K, Arehart E, Hwa J. Versatility and differential roles of cysteine residues in human prostacyclin receptor structure and function. J Biol Chem. 2006; 281:37227–37236. [PubMed: 17015447]
21. Nagahara N, Matsumura T, Okamoto R, Kajihara Y. Protein cysteine modifications: (1) medical chemistry for proteomics. Curr Med Chem. 2009; 16:4419–4444. [PubMed: 19835564]
22. Banerjee A, Ray A, Chang C, Swaan PW. Site-directed mutagenesis and use of bile acid-MTS conjugates to probe the role of cysteines in the human apical sodium-dependent bile acid transporter (SLC10A2). Biochemistry. 2005; 44:8908–8917. [PubMed: 15952798]

23. Al-Ansari N, Xu G, Kollman-Bauerly K, Coppola C, Shefer S, Ujhazy P, Ortiz D, Ma L, Yang S, Tsai R, Salen G, Vanderhoof J, Shneider BL. Analysis of the effect of intestinal resection on rat ileal bile Acid transporter expression and on bile Acid and cholesterol homeostasis. Pediatr Res. 2002; 52:286–291. [PubMed: 12149508]
24. Kramer W, Girbig F, Gutjahr U, Kowalewski S, Jouvenal K, Muller G, Tripier D, Wess G. Intestinal bile acid absorption. Na(+)-dependent bile acid transport activity in rabbit small intestine correlates with the coexpression of an integral 93-kDa and a peripheral 14-kDa bile acid-binding membrane protein along the duodenum-ileum axis. J Biol Chem. 1993; 268:18035–18046. [PubMed: 8349683]
25. Bijsmans IT, Bouwmeester RA, Geyer J, Faber KN, van de Graaf SF. Homo- and hetero-dimeric architecture of the human liver Na(+)-dependent taurocholate co-transporting protein. Biochem J. 2011; 441:1007–1015.
26. Godoy JR, Fernandes C, Doring B, Beuerlein K, Petzinger E, Geyer J. Molecular and phylogenetic characterization of a novel putative membrane transporter (SLC10A7), conserved in vertebrates and bacteria. Eur J Cell Biol. 2007; 86:445–460. [PubMed: 17628207]
27. Fernandes CF, Godoy JR, Doring B, Cavalcanti MC, Bergmann M, Petzinger E, Geyer J. The novel putative bile acid transporter SLC10A5 is highly expressed in liver and kidney. Biochem Biophys Res Commun. 2007; 361:26–32. [PubMed: 17632081]
28. Veenhoff LM, Heuberger EH, Poolman B. Quaternary structure and function of transport proteins. Trends Biochem Sci. 2002; 27:242–249. [PubMed: 12076536]
29. da Silva TC, Hussainzada N, Khantwal CM, Polli JE, Swaan PW. Transmembrane helix 1 contributes to substrate translocation and protein stability of bile acid transporter SLC10A2. J Biol Chem. 286:27322–27332.
30. Craddock AL, Love MW, Daniel RW, Kirby LC, Walters HC, Wong MH, Dawson PA. Expression and transport properties of the human ileal and renal sodium-dependent bile acid transporter. Am J Physiol. 1998; 274:G157–169. [PubMed: 9458785]
31. Yang Y, Liu Y, Dong Z, Xu J, Peng H, Liu Z, Zhang JT. Regulation of function by dimerization through the amino-terminal membrane-spanning domain of human ABCC1/MRP1. J Biol Chem. 2007; 282:8821–8830. [PubMed: 17264072]
32. Yeung YG, Stanley ER. A solution for stripping antibodies from polyvinylidene fluoride immunoblots for multiple reprobing. Anal Biochem. 2009; 389:89–91. [PubMed: 19303392]
33. Gautherot J, Durand-Schneider AM, Delautier D, Delaunay JL, Rada A, Gabillet J, Housset C, Maurice M, Ait-Slimane T. Effects of cellular, chemical, and pharmacological chaperones on the rescue of a trafficking-defective mutant of the ATP-binding cassette transporter proteins ABCB1/ABCB4. J Biol Chem. 2012; 287:5070–5078. [PubMed: 22184139]
34. Smith DF, Whitesell L, Katsanis E. Molecular chaperones: biology and prospects for pharmacological intervention. Pharmacol Rev. 1998; 50:493–514. [PubMed: 9860803]
35. Sabit H, Mallajosyula SS, MacKerell AD Jr, Swaan PW. Transmembrane domain II of the human bile acid transporter SLC10A2 coordinates sodium translocation. J Biol Chem. 2013; 288:32394–32404. [PubMed: 24045943]
36. Henriksen U, Fog JU, Litman T, Gether U. Identification of intra- and intermolecular disulfide bridges in the multidrug resistance transporter ABCG2. J Biol Chem. 2005; 280:36926–36934. [PubMed: 16107343]
37. Leimanis ML, Georges E. ABCG2 membrane transporter in mature human erythrocytes is exclusively homodimer. Biochem Biophys Res Commun. 2007; 354:345–350. [PubMed: 17250810]
38. Luo P, Yu X, Wang W, Fan S, Li X, Wang J. Crystal structure of a phosphorylation-coupled vitamin C transporter. Nat Struct Mol Biol. 2015; 22:238–241. [PubMed: 25686089]
39. Ostuni A, Miglionico R, Monne M, Castiglione Morelli MA, Bisaccia F. The nucleotide-binding domain 2 of the human transporter protein MRP6. J Bioenerg Biomembr. 2011; 43:465–471. [PubMed: 21748403]
40. Visser WE, Philp NJ, van Dijk TB, Klootwijk W, Friesema EC, Jansen J, Beesley PW, Ianculescu AG, Visser TJ. Evidence for a homodimeric structure of human monocarboxylate transporter 8. Endocrinology. 2009; 150:5163–5170. [PubMed: 19797118]

41. Xia X, Roundtree M, Merikhi A, Lu X, Shentu S, Lesage G. Degradation of the apical sodium-dependent bile acid transporter by the ubiquitin-proteasome pathway in cholangiocytes. J Biol Chem. 2004; 279:44931–44937. [PubMed: 15304498]

42. Chothe PP, Swaan PW. Resveratrol promotes degradation of the human bile acid transporter ASBT (SLC10A2). The Biochemical journal. 2014; 459:301–312. [PubMed: 24498857]

43. Javadpour MM, Eilers M, Groesbeek M, Smith SO. Helix packing in polytopic membrane proteins: role of glycine in transmembrane helix association. Biophys J. 1999; 77:1609–1618. [PubMed: 10465772]

44. Kleiger G, Eisenberg D. GXXXG and GXXXA motifs stabilize FAD and NAD(P)-binding Rossmann folds through C(alpha)-H… O hydrogen bonds and van der waals interactions. J Mol Biol. 2002; 323:69–76. [PubMed: 12368099]

45. Senes A, Engel DE, DeGrado WF. Folding of helical membrane proteins: the role of polar, GxxxG-like and proline motifs. Curr Opin Struct Biol. 2004; 14:465–479. [PubMed: 15313242]

46. Duan P, Wu J, You G. Mutational analysis of the role of GXXXG motif in the function of human organic anion transporter 1 (hOAT1). Int J Biochem Mol Biol. 2011; 2:1–7. [PubMed: 21340049]

47. Teese MG, Langosch D. Role of GxxxG Motifs in Transmembrane Domain Interactions. Biochemistry. 2015; 54:5125–5135. [PubMed: 26244771]

48. Wilson MR, Kugel S, Huang J, Wilson LJ, Wloszczynski PA, Ye J, Matherly LH, Hou Z. Structural determinants of human proton-coupled folate transporter oligomerization: role of GXXXG motifs and identification of oligomeric interfaces at transmembrane domains 3 and 6. Biochem J. 2015; 469:33–44. [PubMed: 25877470]

49. Moore RH, Chothe P, Swaan PW. Transmembrane domain V plays a stabilizing role in the function of human bile acid transporter SLC10A2. Biochemistry. 2013; 52:5117–5124. [PubMed: 23815591]

50. Torres GE, Carneiro A, Seamans K, Fiorentini C, Sweeney A, Yao WD, Caron MG. Oligomerization and trafficking of the human dopamine transporter. Mutational analysis identifies critical domains important for the functional expression of the transporter. J Biol Chem. 2003; 278:2731–2739. [PubMed: 12429746]

51. Mo W, Qi J, Zhang JT. Different roles of TM5, TM6, and ECL3 in the oligomerization and function of human ABCG2. Biochemistry. 2012; 51:3634–3641. [PubMed: 22497316]

52. Yang Y, Mo W, Zhang JT. Role of transmembrane segment 5 and extracellular loop 3 in the homodimerization of human ABCC1. Biochemistry. 2010; 49:10854–10861. [PubMed: 21090806]

53. Hu NJ, Iwata S, Cameron AD, Drew D. Crystal structure of a bacterial homologue of the bile acid sodium symporter ASBT. Nature. 2011; 478:408–411. [PubMed: 21976025]

54. Zhou X, Levin EJ, Pan Y, McCoy JG, Sharma R, Kloss B, Bruni R, Quick M, Zhou M. Structural basis of the alternating-access mechanism in a bile acid transporter. Nature. 2014; 505:569–573. [PubMed: 24317697]

55. Lionarons DA, Boyer JL, Cai SY. Evolution of substrate specificity for the bile salt transporter ASBT (SLC10A2). J Lipid Res. 2012; 53:1535–1542. [PubMed: 22669917]

Research Highlights

- Formation of dimeric or higher order multimeric assemblies of hASBT is proposed
- Dimers and oligomers of hASBT are functionally active
- Self-association of this protein does not rely on cysteine residues
- Cysteine-free hASBT acts as a dominant negative construct, but associates with wild-type hASBT at the membrane surface

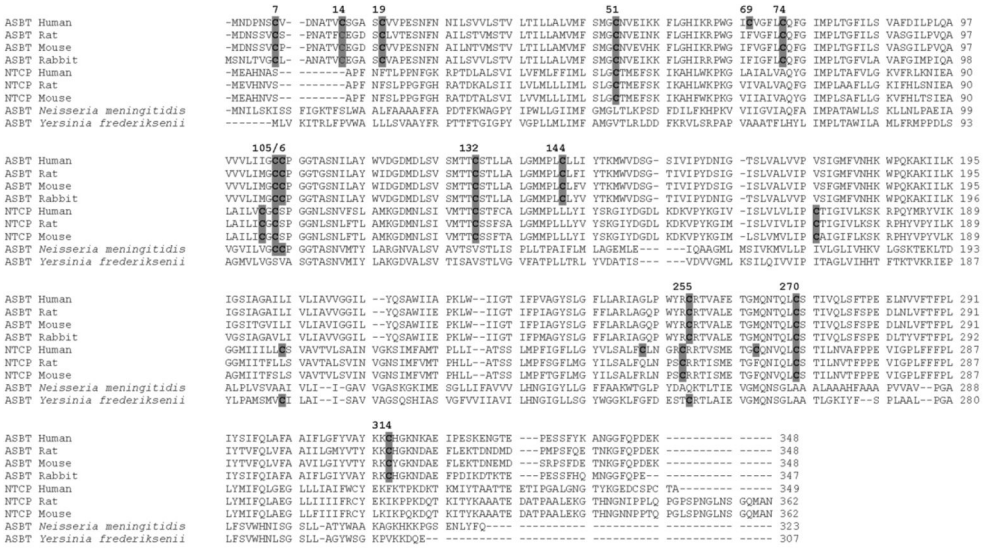

Figure 1.

Multiple protein sequence alignment of ASBT (*SLC10A2*). Protein sequences were retrieved from GenBank in FASTA format and aligned via ClustalW2 with manual adjustment. ASBT, apical sodium-dependent bile transporter; NTCP, Na^+-taurocholate cotransporting polypeptide (*SLC10A1*).

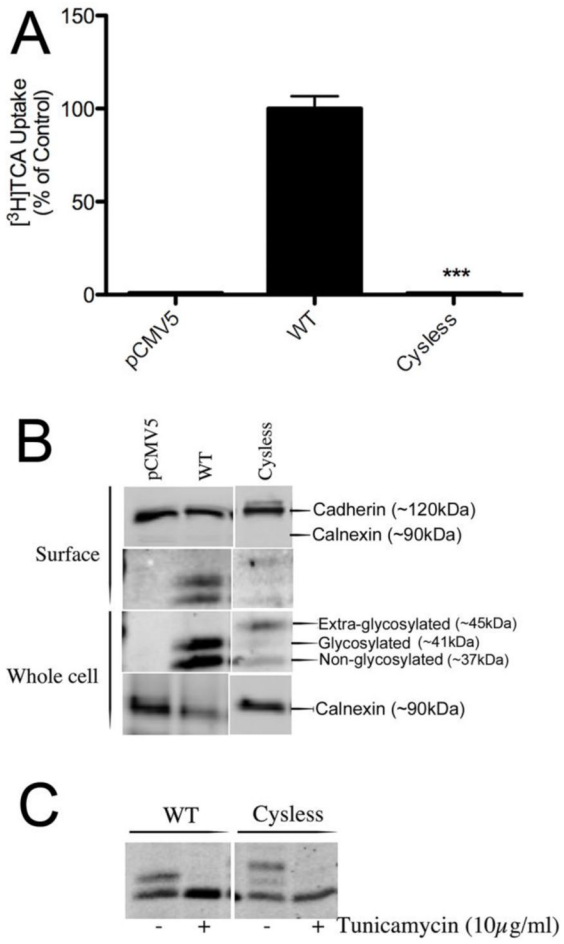

Figure 2.

Transport activity and membrane expression of Cysless hASBT. **(A)** COS-1 cells were transfected with WT and Cysless hASBT followed by [^{3}H]-TCA uptake as described under 'Materials and Methods'. Uptake activity for Cysless hASBT is represented as a percent of WT hASBT control. Initial uptake rates were normalized with respective membrane expression. **(B)** Total (whole cell) and surface (biotinylation) protein expression of WT and Cysless hASBT. Equal amount of protein was (20 μg) loaded for both WT and Cysless hASBT and separated on 10% SDS-PAGE. Cell surface protein labeling selectivity was confirmed by the absence of ER protein calnexin (~ 90 kDa, mouse anti-calnexin 1:1000) and the presence of cell surface marker pan-cadherin (~ 120 kDa, rabbit anti-cadherin 1:2000). Mature glycosylated hASBT visualizes as the glycosylated (~41 kDa) and non-glycosylated (~37 kDa) band. An extra glycosylated band was also observed for Cysless hASBT (~45 kDa). Blots are representative of two independent experiments. **(C)** COS-1 cells were transiently transfected with WT and Cysless hASBT as described under 'Materials and Methods'. 48 h post-transfection cells were treated with tunicamycin (10μg/ml) for 24 h followed by Western blot analysis using goat anti-hASBT antibody. The blots shown in Figure 1B and C are from the same experiment. The actual blot needed to be cut to join the band representing Cysless hASBT protein with WT band. ***$p<0.001$, statistical significance.

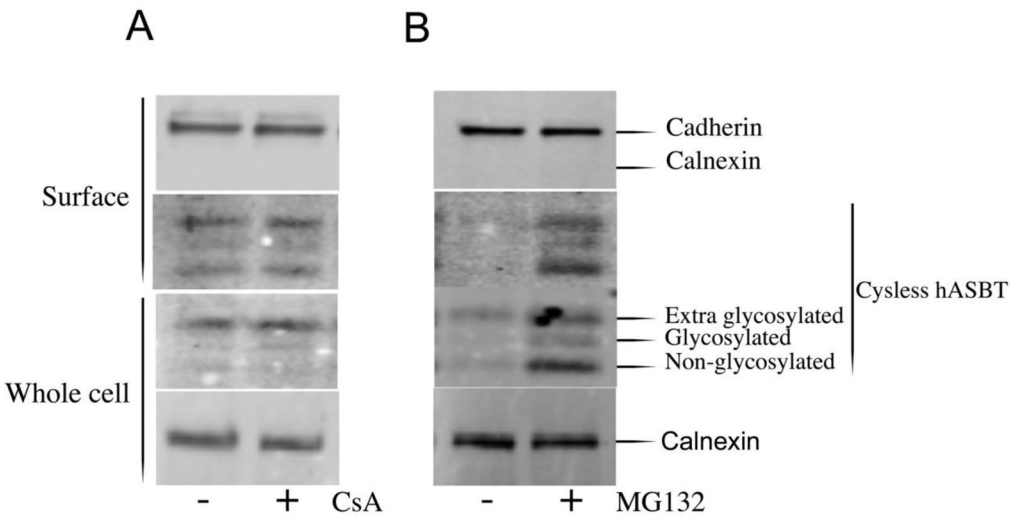

Figure 3.

Effect of cyclosporin A and MG132 on membrane expression of Cysless hASBT.

COS-1cells were transfected with Cysless hASBT as described under ‘Materials and Methods’. After 48 h, cells were treated with **(A)** cyclosporin A (25 μM) for 18 h and **(B)** MG132 (10 μM) for 6 h followed by surface biotinylation and Western blot analysis as described under ‘Materials and Methods’ using goat anti-hASBT antibody. Pan-cadherin was used as a cell surface marker while calnexin served as a control for whole cell lysate.

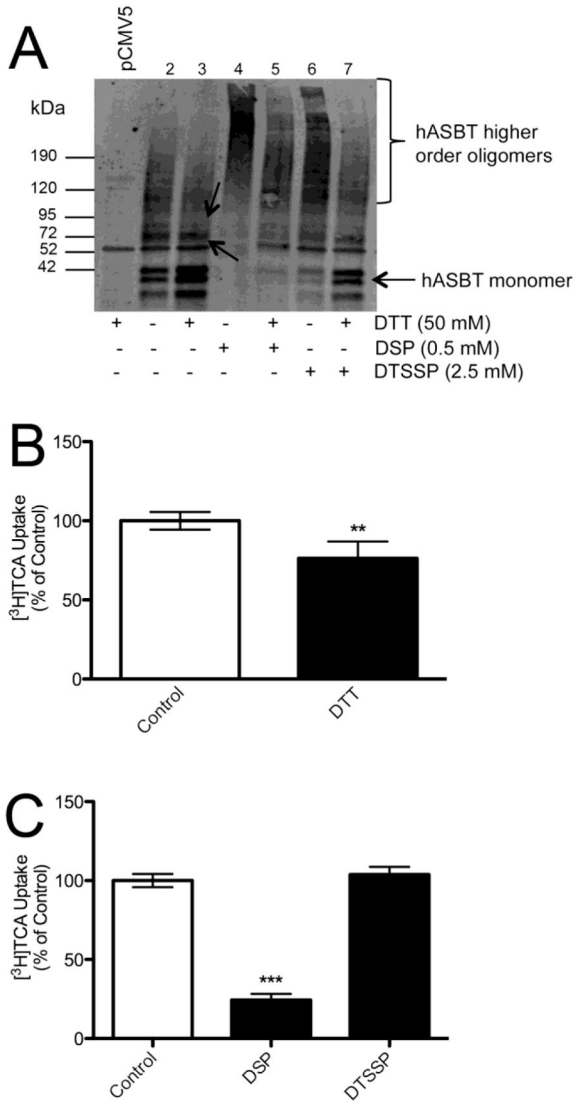

Figure 4.

Chemical cross-linking of wt-hASBT with DSP and DTSSP under reducing and non-reducing conditions (DTT+/−). (A) COS-1 cells were transiently transfected with pCMV5 vector control (lane 1) and wt-hASBT (lanes 2–7) as described under ‘Materials and Methods’. 48 h post-transfection, cells were incubated with and without DSP (0.5 mM) and DTSSP (2.5 mM) for 30 min at room temperature as indicated by + and − signs in the table underneath the blot. Cell lysates were prepared for separation by 4–15% SDS-PAGE in the absence and presence of 50 mM DTT followed by Western blot analysis using goat anti-hASBT (1:1000) antibody. Upper and lower arrows shown in lane 3 (labeled 1 and 2) indicate the glycosylated and non-glycosylated forms of hASBT, respectively.

(B) hASBT transfected COS-1 cell were pre-incubated with DTT (10 mM) for 30 min followed by [^{3}H]-TCA uptake. Initial uptake rates were calculated and presented as percent control (no treatment). **(C)** COS-1 cells overexpressing hASBT were treated with DSP (0.5 mM) and DTSSP (2.5 mM) for 30 min followed by [^{3}H]-TCA uptake analysis. Statistical analysis was done with ANOVA with Dunnett’s post hoc test to see the difference in the

uptake in the absence and presence of DSP and DTSSP. Data are represented as a percent of control (no treatment). *** $P < 0.001$ and ** $P < 0.01$.

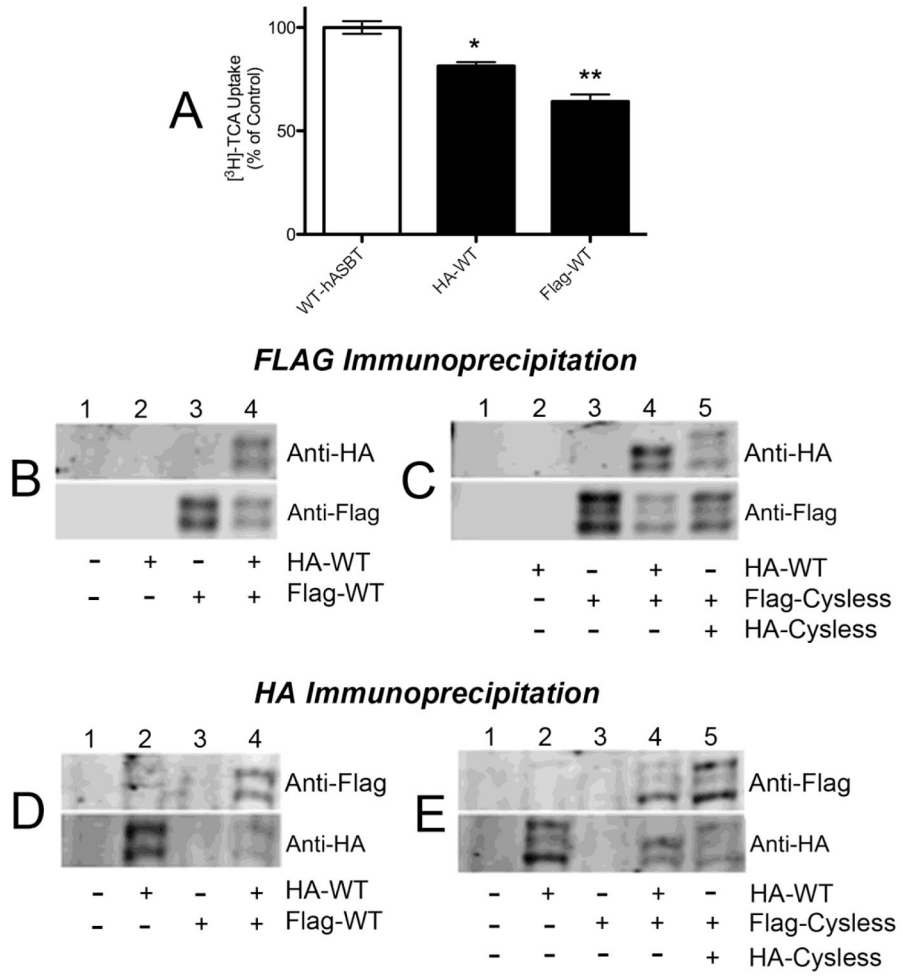

Figure 5.

Homodimerization of hASBT. **(A)** Functional analysis of HA and Flag tagged hASBT. COS-1 cells were transiently transfected with HA and Flag-hASBT and used for [^{3}H]-TCA uptake as described in ‘Materials and Methods’. Data are represented as percent control (WT hASBT). **(B)** Co-immunoprecipitation of differentially tagged hASBT. COS-1 cells were transiently transfected with HA-hASBT (lane 2), Flag-hASBT (lane 3) alone and together (lane 4). **(C)** COS-1 cells were transiently transfected with HA-WT (lane 2), Flag-Cysless (lane 3) alone or HA-WT with Flag-Cysless (lane 3) and HA-Cysless with Flag-Cysless (lane 4). IgG served as a control (lane 1). Cells were harvested and lysates were prepared for immunoprecipitation by anti-Flag antibody as described under ‘Materials and Methods’. The immunoprecipitates were then separated on 10% SDS-PAGE followed by Western blot analysis using mouse anti-HA antibody (B and C, top panels). The blots were stripped as described under ‘Materials and Methods’ and then reprobed with mouse anti-Flag antibody for input analysis (B and C, bottom panels). **(D), (E)** The lysates from previous experiment (B and C) were used for immunoprecipitation using mouse anti-HA antibody. Immunoprecipitates were separated by 10% SDS-PAGE followed Western blotting with mouse anti-Flag antibody (D and E, top panels). The blots were stripped and then

reprobed with mouse anti-HA antibody for input analysis (D and E, bottom panels). *$p<0.05$ and **$p<0.01$.

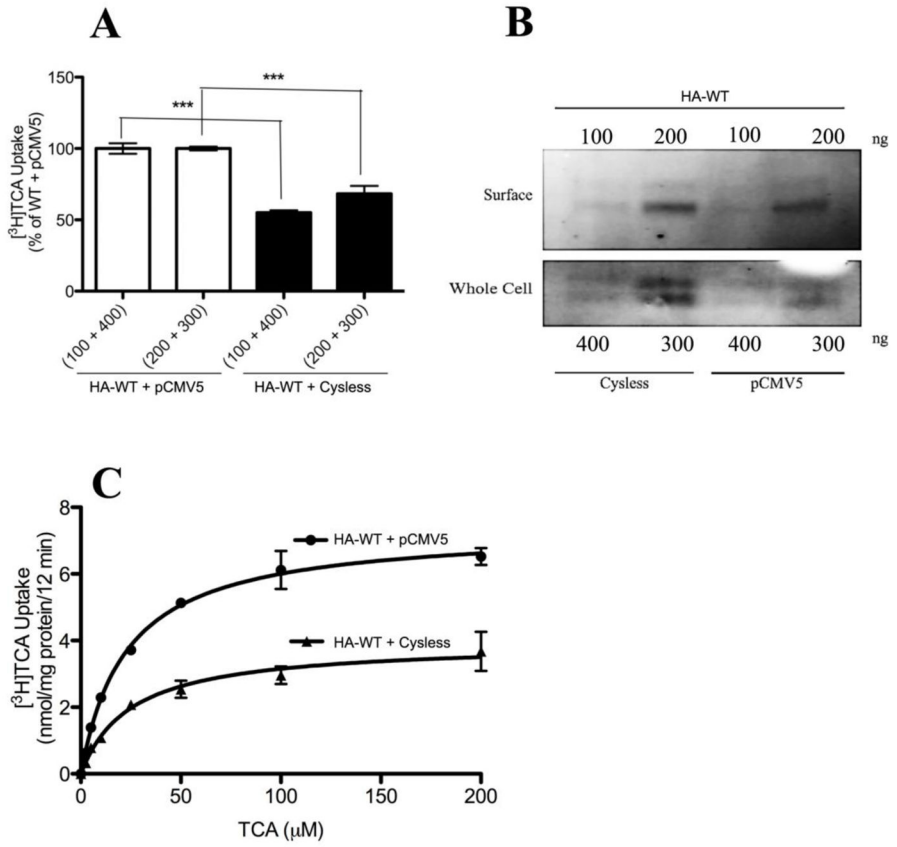

Fig. 6.

Functional evidence for the oligomerization of HA-WT hASBT when co-expressed with Cysless hASBT. **(A)** COS-1 cells were co-transfected with either HA-WT and pCMV5 or HA-WT and Cysless hASBT at indicated concentrations. [^{3}H]-TCA uptake was performed 48 h post-transfection. The uptake rates were normalized with the HA-WT surface expression. Data is represented as a percent of control uptake (HA-WT and pCMV5). **(B)** Surface biotinylation of HA-WT co-expressed with either pCMV5 or Cysless hASBT. HA-WT was co-expressed with either pCMV5 or Cysless hASBT followed by surface biotinylation and Western blot analysis as described under 'Materials and Methods'. **(C)** Kinetic analysis of HA-WT in the presence of Cysless hASBT. COS-1 cells were co-transfected with HA-WT along with either Cysless hASBT or pCMV5 at ratio of 200:300 (HA-WT:pCMV5/Cysless). 48h post-transfection, [^{3}H]-TCA uptake was measured for 12 min in MHBSS buffer at increasing concentration of unlabeled TCA (2.5 – 200 μM). Radiolabeled [^{3}H]-TCA was used as a tracer (1μCi/ml). Uptake rates were normalized with HA-WT surface expression as described in figure 6B. Kinetic parameters K_t and V_{max} were determined as indicated in 'Materials and Methods'. ***$p < 0.001$.